

Pre-saddle neutron multiplicity for fission reactions induced by heavy ions and light particles

S. Soheyli* and M. K. Khalili

Department of Physics, Bu-Ali Sina University, Hamedan, Iran

(Received 3 August 2012; revised manuscript received 25 December 2012; published 7 March 2013)

Pre-saddle neutron multiplicity has been calculated for several fission reactions induced by heavy ions and light particles. Experimentally, it is impossible to determine the contribution of neutrons being emitted before the saddle point and those emitted between the saddle and the scission points. Determination of the pre-saddle neutron multiplicity in our research is based on the comparison between the experimental anisotropies and those predicted by the standard saddle-point statistical model. Analysis of the results shows that the pre-saddle neutron multiplicity depends on the fission barrier height and stability of the compound nucleus. In heavy-ion-induced fission, the number of pre-saddle neutrons decreases with increasing excitation energy of the compound nucleus. A main cause of this behavior is due to a reduction in the ground-state-to-saddle-point transition time with increasing excitation energy of the compound nucleus. However, in induced fission by light particles, the number of pre-saddle neutrons increases with increasing excitation energy of the compound nucleus.

DOI: [10.1103/PhysRevC.87.034610](https://doi.org/10.1103/PhysRevC.87.034610)

PACS number(s): 25.70.Jj, 25.85.Ge

I. INTRODUCTION

Over the last two decades, much theoretical attention has been directed towards understanding the dynamics of fission. According to reports, measuring the number of neutrons emitted during fission most likely gives information on the time scale of fission as well as on the nuclear dynamics. The transition state model of fission, based on appropriate level densities, predicts the widths (and thus lifetimes) of fission and neutron emission. This model is also suitable for determining the pre-fission neutron multiplicity if the calculated lifetimes are long compared to the dynamically constrained fission lifetime. Several groups have invested an extensive effort in measuring the number of emitted neutrons associated with fission reactions induced by heavy ions [1–17]. The measurement of emitted neutrons is usually limited to the measurement of pre-scission neutron multiplicity, post-scission neutron multiplicity, and therefore total neutron multiplicity. These measurements show that the transition state model of fission leads to an underestimation of the number of measured pre-scission neutrons emitted in heavy-ion-induced fission at high excitation energies. This discrepancy can be related to the viscosity of the hot nucleus [18]. Hence, the fission lifetime of a hot nucleus is substantially longer than that determined by the statistical model of Bohr and Wheeler [19]. As a result, it is natural to expect that a dissipative dynamical model would provide an appropriate description of nuclear fission at high excitation energies [20].

Pre-scission neutrons ν_{pre} can be emitted between the ground state of the compound nucleus and the saddle point (pre-saddle neutrons) ν_{gs} or between the saddle and the scission points (saddle-to-scission neutrons) ν_{ss} . The number of pre-saddle neutrons as well as the number of saddle-to-scission neutrons can be determined by a combined dynamical statistical model (CDSM) [21–23]. The contributions ν_{gs} and ν_{ss} to the pre-scission neutron multiplicity are also estimated

by a stochastic approach based on a three-dimensional Langevin equation [24]. Recently, a more accurate four-dimensional Langevin model, an extension of the three-dimensional Langevin model by adding the fourth collective coordinate (the projection of the total spin about the symmetry axis of the fissioning nucleus), was used to calculate the pre-scission neutron multiplicity [25].

A common assumption in the calculation of the angular anisotropy of fission fragments using the transition state model is that all pre-scission neutrons are emitted prior to reaching the saddle point since it is not straightforward to separate experimentally the contribution of neutrons being emitted before the saddle point and those emitted between the saddle and the scission points [26–35]. It is well known that the standard saddle-point statistical model (SSPSM) has become the standard theory of fission-fragment angular distributions and has had great success since it was proposed. The effect of neutron evaporation prior to reaching the saddle point is to reduce the temperature of the fissioning nucleus, which in turn increases the fission-fragment anisotropy prediction by using this model. Only ν_{gs} has an influence over the prediction of angular anisotropy by using SSPSM. The upper limit of the angular anisotropy of fission fragments, based on the prediction of SSPSM, is determined by assuming that all the pre-scission neutrons are emitted before the saddle point.

The pre-saddle neutrons as a crucial quantity in determining the angular anisotropy of fission fragments by using SSPSM play the main role, although no precise method to determine the pre-saddle neutrons has been introduced. In this article, we calculate the number of pre-saddle neutrons by a novel method. In this method, the values of ν_{gs} for several fission reactions induced by light particles and heavy ions are determined by the fission-fragment angular distribution method. This method is based on a comparison between the experimental anisotropies and those predicted by the standard saddle-point statistical model. This method is limited to the calculation of pre-saddle neutrons in induced fission in which the angular anisotropy of fission fragments has a normal behavior; i.e., a good agreement is observed between the angular anisotropy of fission fragments and that predicted by the SSPSM.

* Corresponding author: s.soheyli@basu.ac.ir

In order to make the present paper self-contained, we present in Sec. II a brief description of the standard saddle-point statistical model as well as the details of the calculation method of the pre-saddle neutron multiplicity on the basis of the SSPSM. Section III is devoted to the results obtained in this study. Finally, the concluding remarks are given in Sec. IV.

II. METHOD OF CALCULATIONS

A. Standard saddle-point statistical model

The standard transition-state model has been used to analyze the angular anisotropy of fission fragments in fission. In the transition-state model, the equilibrium distribution over the K degree of freedom (the projection of total angular momentum of the compound nucleus I on the symmetry axis of the fissioning nucleus) is assumed to be established at the transition state. Two versions of the transition-state model based on assumptions about the position of the transition state, the SSPSM and the scission-point statistical model (SPSM), can be used to predict fission-fragment angular distributions. The basic assumption of the SSPSM is that fission proceeds along the symmetry axis of a deformed compound nucleus and that the distribution of K is frozen from the saddle point to the scission point. In this model, the fission-fragment angular distribution $W(\theta)$ for the fission of spin-zero nuclei is given by the following expression [36]:

$$W(\theta) \propto \sum_{I=0}^{\infty} \frac{(2I+1)^2 T_I \exp[-p \sin^2 \theta] J_0[-ip \sin^2 \theta]}{\text{erf}[\sqrt{2p}]}, \quad (1)$$

where T_I and J_0 are the transmission coefficients for fission and the zeroth-order Bessel function, $p = (I + \frac{1}{2})^2 / (4K_o^2)$, and the variance of the equilibrium K distribution (K_o) is

$$K_o^2 = \frac{\mathfrak{S}_{eff} T}{\hbar^2}. \quad (2)$$

Here \mathfrak{S}_{eff} and T are the effective moment of inertia and the nuclear temperature of the compound nucleus at the saddle point, respectively.

The angular anisotropy of fission fragments is defined as

$$A = \frac{W(0^\circ)}{W(90^\circ)}. \quad (3)$$

The nuclear temperature of the compound nucleus at the saddle point is given by

$$T = \sqrt{\frac{E_{ex}}{a}}, \quad (4)$$

where E_{ex} is the excitation energy of the fissioning system and a is the nuclear level-density parameter at the saddle point. E_{ex} can be expressed by the following relation:

$$E_{ex} = E_{c.m.} + Q - B_f(I) - E_R(I) - \nu_{gs} E_n. \quad (5)$$

In this equation, $E_{c.m.}$, Q , $B_f(I)$, $E_R(I)$, ν_{gs} , and E_n represent the center-of-mass energy of the projectile, the Q value, the spin-dependent fission barrier height, the spin-dependent rotational energy of the compound nucleus, the number of

pre-saddle neutrons, and the average excitation energy lost due to evaporation of one neutron from the compound nucleus prior to the system reaching the saddle point, respectively. In the case of $p \gg 1$, the angular anisotropy of fission fragments by using Eq. (1) is given by the following approximate relation:

$$A \approx 1 + \frac{\langle I^2 \rangle}{4K_o^2}. \quad (6)$$

The prediction of angular anisotropy of fission fragments using the SSPSM is valid only under restrictive assumptions. At high angular momentum or at high fissility, the rotating liquid drop model (RLDM) predicts that the fission barrier height $B_f(I)$ vanishes even for a spherical nucleus, which leads to $K_o^2 \rightarrow \infty$. Subsequently, the distribution of K is uniform, and hence the prediction of the SSPSM for the fission-fragment angular anisotropy is nearly uniform using Eq. (1). This predicted tendency toward isotropy for fission fragments at high angular momentum is not seen in the experiments. This discrepancy is taken as a clear indication that the width of the K distribution is not determined at the predicted spherical saddle-point shape but at a point where the nucleus is more deformed. Therefore it has been proposed that the standard saddle-point statistical model breaks down at high spin and/or large values of $\frac{Z^2}{A}$ of the compound nucleus (CN), and the angular distribution of fission fragments is governed by an effective transition state different from the saddle-point transition state.

B. Pre-saddle neutron multiplicity

It is clear that because of the hindrance to fission, a large number of particles, more than predicted by the statistical model, are emitted from the fissioning system. In heavy-ion fusion reactions, due to the formation of a heavy compound nucleus, the competition between neutron emission and fission describes the decay possibilities rather well. During the collective motion to the scission point, neutrons will be evaporated if energetically possible, and would behave experimentally as pre-fission, or more correctly, pre-scission neutrons. A longer saddle to scission time due to the viscosity effect will result in a higher pre-scission neutron multiplicity [15]. The calculation of pre-saddle neutrons in heavy-ion-induced reactions based on the comparison of the experimental data of angular anisotropy with those predicted by the SSPSM depends on the kinetic energy and the binding energy of the neutron evaporated from the compound nucleus prior to the system reaching the saddle point. The energy spectrum of evaporated neutrons is usually given by the following form (an evaporation spectrum) [37]:

$$\frac{dN}{dE} = CE \exp\left(-\frac{E}{T}\right). \quad (7)$$

Hence, the average kinetic energy of the emitted neutron \bar{E}_K is given by

$$\bar{E}_K = 2T. \quad (8)$$

The average excitation energy lost due to evaporation of one neutron from the compound nucleus prior to the system reaching the saddle point is given by

$$E_n = B_n + 2T, \quad (9)$$

where B_n denotes the average neutron separation energy.

In this work, the average energy lost by an emitted neutron over the energy range of the projectile is calculated by Eq. (9) for heavy-ion-induced fission reactions, as well as for fissions induced by light projectiles. The level-density parameter a is taken as $\frac{A_{C.N.}}{8}$. (Considering the level-density parameter as $\frac{A_{C.N.}}{10}$, rather than $\frac{A_{C.N.}}{8}$, the number of pre-saddle neutrons varies at most by 10%.) Hence, the number of pre-saddle neutrons is not sensitive to the level-density parameter selected in the calculation. \mathfrak{S}_{eff} , $B_f(I)$, and $E_R(I)$ are accounted for by the use of the rotating finite-range model (RFRM) [38], while $\langle I^2 \rangle$ quantities are calculated by several models [39–44]. In the following sections, the determination of the number of pre-saddle neutrons ν_{gs} for these systems is based on the comparison between the experimental data of angular anisotropies and those predicted by the SSPSM. In the present work, we determine pre-saddle neutron multiplicities for several systems undergoing heavy-ion-induced fission in which fission-fragment angular anisotropies have a normal behavior as well as those systems undergoing light-particle-

induced fission. In order to determine the number of pre-saddle neutrons in heavy-ion reactions with anomalous angular anisotropies, it is necessary to predict the average contribution of noncompound nucleus fission events [45].

III. RESULTS AND DISCUSSION

The calculated multiplicities of pre-saddle neutrons as a function of E_{ex} for the $^{16}\text{O} + ^{209}\text{Bi} \rightarrow ^{225}\text{Pa}$ and $^{19}\text{F} + ^{208}\text{Pb} \rightarrow ^{227}\text{Pa}$ reaction systems leading to protactinium isotopes are shown in Fig. 1(a). For the above studied systems, the experimental data of angular anisotropy are taken from the literature [46,47]. As illustrated in Fig. 1(a), the number of pre-saddle neutrons decreases with increasing excitation energy of the compound nucleus. This behavior is due to the fact that the fission barrier height (and thus the ground-state-to-saddle-point transition time) decreases with increasing excitation energy of the compound nucleus, which can lead to ν_{gs} decreasing with E_{ex} . In Fig. 1(a), the general trend of the number of pre-saddle neutrons as a function of the excitation energy of the compound nucleus is represented by a line using the method of least squares. Figure 1(b) shows a similar case for the $^{16}\text{O} + ^{208}\text{Pb} \rightarrow ^{224}\text{Th}$ reaction system. For this system, the experimental data of angular anisotropy are taken from the literature [8]. Multiplicities of pre-saddle neutrons for the $^{11}\text{B} + ^{237}\text{Np}$ and $^{16}\text{O} + ^{232}\text{Th}$ reaction systems, both

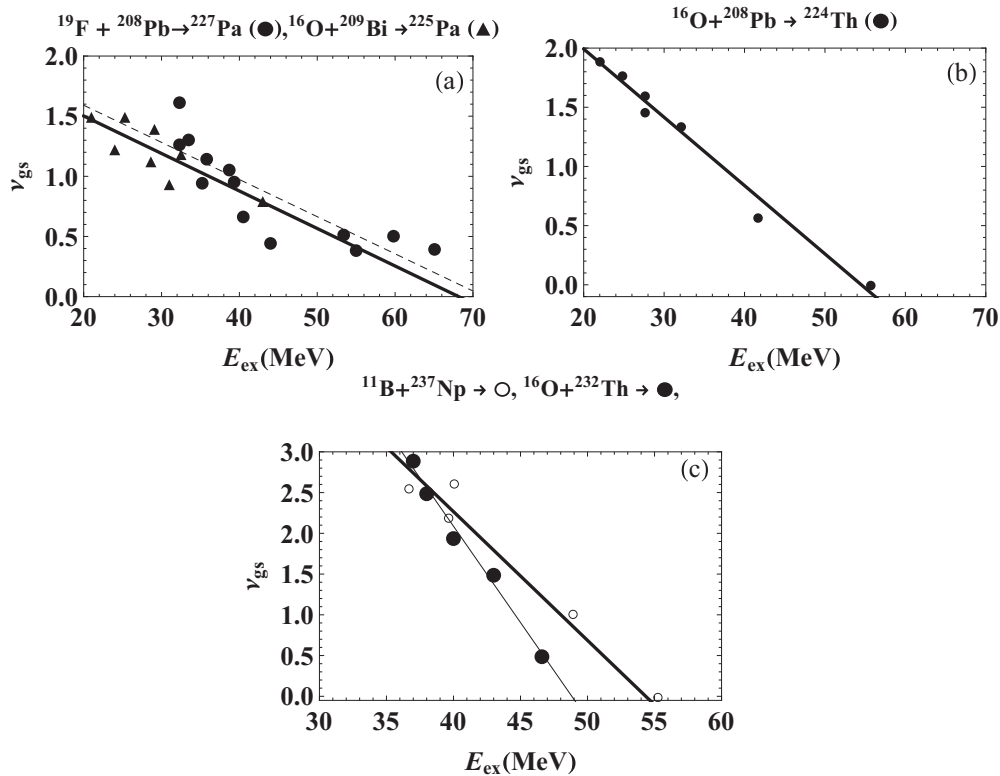


FIG. 1. Calculated multiplicities of pre-saddle neutrons. (a) For the $^{16}\text{O} + ^{209}\text{Bi} \rightarrow ^{225}\text{Pa}$ and $^{19}\text{F} + ^{208}\text{Pb} \rightarrow ^{227}\text{Pa}$ reaction systems. Solid and dashed lines represent the general trends of ν_{gs} against the excitation energy of the compound nucleus for the $^{16}\text{O} + ^{209}\text{Bi} \rightarrow ^{225}\text{Pa}$ and $^{19}\text{F} + ^{208}\text{Pb} \rightarrow ^{227}\text{Pa}$ reaction systems, respectively. (b) For the $^{16}\text{O} + ^{208}\text{Pb} \rightarrow ^{224}\text{Th}$ reaction system. The solid line represents the general trend of ν_{gs} against the excitation energy of the compound nucleus. (c) For the $^{11}\text{B} + ^{237}\text{Np}$ and $^{16}\text{O} + ^{232}\text{Th}$ reaction systems, both populating the same compound nucleus ^{248}Cf . Thick and thin lines represent the general trends of ν_{gs} against the excitation energy of the compound nucleus for the $^{11}\text{B} + ^{237}\text{Np}$ and $^{16}\text{O} + ^{232}\text{Th}$ reaction systems, respectively.

TABLE I. Comparison between the calculated v_{cal}^{gs} , $v_{cal}^{gs}/v_{exp}^{pre}$, and v_{th}^{gs}/v_{th}^{pre} [21] for the $^{16}\text{O} + ^{208}\text{Pb} \rightarrow ^{224}\text{Th}$ reaction system.

$E_{c.m.}$ (MeV)	E_{ex} (MeV)	v_{exp}^{pre}	v_{cal}^{gs}	$v_{cal}^{gs}/v_{exp}^{pre}$	v_{th}^{gs}/v_{th}^{pre}
76.9	22.7	1.50	1.81	1.21	0.96
82.6	27.6	1.90	1.60	0.84	0.91
92.0	32.0	2.40	1.30	0.54	0.78
105.9	42.5	2.80	0.52	0.18	0.64
119.0	55.0	3.40	0.00	0.00	0.56

populating the same compound nucleus ^{248}Cf , are shown in Fig. 1(c). For these two systems, the experimental data of $\langle A \rangle$ are taken from the literature [48–50]. It is interesting to note that for these two systems, as well as for the $^{16}\text{O} + ^{209}\text{Bi} \rightarrow ^{225}\text{Pa}$ and $^{19}\text{F} + ^{208}\text{Pb} \rightarrow ^{227}\text{Pa}$ reaction systems as shown in Fig. 1(a), the number of pre-saddle neutrons at any given excitation energy appears to be nearly equal. As a result, the multiplicities of pre-saddle neutrons for heavy-ion fusion reactions populating the same compound nucleus are nearly independent of the entrance channel asymmetry and depend on the mass number of the compound nucleus.

The ratio of the calculated pre-saddle neutron multiplicity v_{cal}^{gs} to experimental pre-scission neutron multiplicity v_{exp}^{pre} [8] and also the ratio of theoretical pre-saddle neutron multiplicity to theoretical pre-scission neutron multiplicity [21] for the $^{16}\text{O} + ^{208}\text{Pb} \rightarrow ^{224}\text{Th}$ reaction system are given in Table I. As can be seen from Table I, the calculated number of pre-saddle neutrons for the $^{16}\text{O} + ^{208}\text{Pb} \rightarrow ^{224}\text{Th}$ reaction system is greater than v_{exp}^{pre} at $E_{c.m.} = 76.9$ MeV. This unexpected result can be related to the measured value of fission-fragment angular anisotropy at low energy. It seems that the measured value of the angular anisotropy at $E_{c.m.} = 76.9$ MeV is overestimated.

As the nucleus is heated, the excitation energy of the compound nucleus E_{ex} exceeds the fission barrier height B_f . Hence it becomes possible for the nucleus to fission after passing through excited states above the fission barrier (transient state) [51]. In this transient-state picture, the fission width Γ_f depends on the level density above the fission barrier. The fission width and the neutron width can be shown to be approximately given by $\Gamma_f \propto \exp(-\frac{B_f}{T})$ and $\Gamma_n \propto \exp(-\frac{B_n}{T})$ (B_n is the neutron binding energy), respectively. Therefore, the energy dependence of the ratio $\frac{\Gamma_n}{\Gamma_f}$ is expected to be dominated by the ratio of appropriate Boltzmann factors, i.e., $\frac{\Gamma_n}{\Gamma_f} \approx \exp[(B_f - B_n)/T]$.

In general, in heavy-ion-induced fission, B_f will be relatively high at low excitation energy or at low angular momentum I ; however as I , as well as E_{ex} , is increased, the larger moment of inertia of the elongated saddle point configuration causes its energy to increase less rapidly than that of the compact equilibrium deformation, so the barrier height falls to zero at some I . The ratio $\frac{\Gamma_n}{\Gamma_f}$ is known to decrease sharply as E_{ex} increases in the nuclei of the lead-bismuth region, and it is expected to do just the opposite for nuclei with the largest known atomic numbers [52]. For the lighter group of fissioning elements, $B_f \gg B_n$, and for the very heavy ones, it is expected that $B_n \gg B_f$. For nuclei of intermediate mass

like neptunium, B_n and B_f are nearly equal, and one expects only a slow variation of $\frac{\Gamma_n}{\Gamma_f}$ with E_{ex} . In a heavy-ion reaction, there is sufficient excitation energy to emit several neutrons, and fission can compete at each stage (if the excitation energy is greater than the fission barrier height); thus the fission probability and neutron evaporation probability at stage i are given by $p_{f,i} = (\frac{\Gamma_f}{\Gamma_{tot}})_i$ and $p_{n,i} = (\frac{\Gamma_n}{\Gamma_{tot}})_i = 1 - (\frac{\Gamma_f}{\Gamma_{tot}})_i$, respectively. As a result, the total fission probability P_f is given by

$$P_f = \sum_{k=1}^v \prod_{i=1}^k (p_{f,i})(p_{n,i-1}), \quad (10)$$

where $\Gamma_{tot} = \Gamma_f + \Gamma_n$. The mean number of neutrons emitted before fission v_{pre} can be derived by the following expression:

$$v_{pre} = \left(\frac{1}{P_f}\right) \sum_{k=1}^v (k-1) \prod_{i=1}^k (p_{f,i})(p_{n,i-1}). \quad (11)$$

As I increases, the fission barrier height decreases; then $p_{f,i}$ along the decay chain approaches unity, steps with $k > 1$ become insignificant, and $v_{pre} \rightarrow 0$. Thus fission is predicted to occur at the first step in the decay chain. It is obvious that as the projectile energy rises, v_{pre} will initially rise due to a greater number of chances for fission but should subsequently fall as the angular momentum reaches the value at which P_f nears unity. It is shown that the transient time at the scission point τ_{sci} using a diffusion model for the fission process is given by [53]

$$\tau_{sci} \simeq \tau_{sad} + \bar{\tau} = \beta^{-1} \ln(10B_f/T) + \bar{\tau}, \quad (12)$$

where τ_{sad} , $\bar{\tau}$, and β are the transient time at the saddle point, the average traveling time between the saddle and scission points, and the nuclear friction, respectively. The time $\bar{\tau}$ is a function of the value of the nuclear friction, of the shape of potential, and of the excitation energy. The above equation shows that τ_{sad} depends sensibly on the nuclear friction β and on the excitation energy of the compound nucleus.

Earlier calculations of fission-fragment anisotropies based on SSPSM have been corrected to include the effect of pre-scission neutron emission. The calculation of fission-fragment anisotropies with taking into account the effect of pre-scission neutron emission better compares with the SSPSM predictions with the experimental results. However, there is a small discrepancy between model predictions and the data at high excitation energies. A fraction of pre-scission neutrons is expected to be emitted between the saddle and scission. These latter neutrons do not longer influence the prediction of angular anisotropy by SSPSM since it is assumed that the SSPSM is decided at the saddle point. In Fig. 2, the effect of pre-saddle neutrons in the prediction of angular anisotropy by SSPSM is demonstrated for the $^{16}\text{O} + ^{208}\text{Pb} \rightarrow ^{224}\text{Th}$ reaction system [21]. As shown in Fig. 2, the discrepancy between the experimental data of angular anisotropies and the prediction of the SSPSM can be removed to a large extent by taking into account the pre-saddle neutron emission correction. We observe that for the above studied system, the ratio of the calculated pre-saddle neutron multiplicity to experimental pre-scission neutron multiplicity, $v_{cal}^{gs}/v_{exp}^{pre} \approx \frac{1}{4.1}$

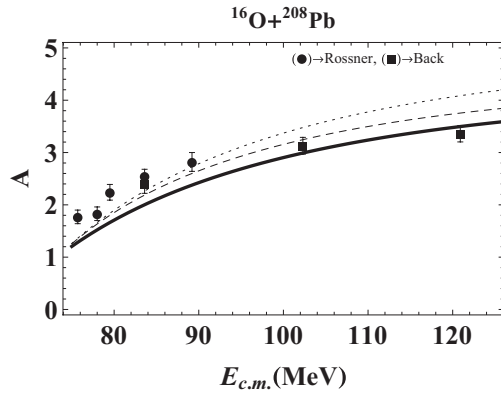


FIG. 2. Experimental and calculated anisotropies in the $^{16}\text{O} + ^{208}\text{Pb} \rightarrow ^{224}\text{Th}$ reaction system [8,57]. Solid, dashed, and dotted curves are the theoretical analysis in the framework of the SSPSM without neutron emission correction, with pre-saddle neutron correction [$v_{exp}^{pre}(v_{th}^{gs}/v_{th}^{pre})$], and with pre-scission neutron correction [v_{exp}^{pre}], respectively.

at $\frac{B_f}{T} = 1$, is in agreement with $\frac{\tau_{gs}}{\tau_{gs} + \tau_{ss}} \approx \frac{1}{3.7}$ (where τ_{gs} and τ_{ss} are ground-to-saddle and saddle-to-scission transition times, respectively) [9]. Hence, the neutron emission rate by the

compound nucleus in the transition from the ground state to the saddle point and then in the transition from the saddle to the scission points are approximately uniform.

The calculated multiplicities of pre-saddle neutrons as a function of E_{ex} for the $^{11}\text{B} + ^{197}\text{Au}$, ^{209}Bi , ^{235}U , ^{237}Np reaction systems are shown in Fig. 3(a). For these studied systems, the experimental data of the angular anisotropies are taken from the literature [46,48,54–58]. The values of ν_{gs} as a function of E_{ex} for the ^{14}N , $^{16}\text{O} + ^{197}\text{Au}$ and ^{14}N , $^{16}\text{O} + ^{209}\text{Bi}$ reaction systems are shown in Fig. 3(b). For these systems, the experimental data of angular anisotropies are taken from the literature [46,47]. The calculated multiplicities of pre-saddle neutrons as a function of the excitation energy of the compound nucleus for induced fission of the ^{209}Bi target by using different projectiles are shown in Fig. 3(c).

The average values of ν_{gs} , as well as ranges of pre-saddle neutron multiplicities for the fission reactions of different targets induced by the same projectile over the same projectile energy range, are shown in Table II. In Table II, the quantity V_b denotes the Coulomb barrier height. It can be observed that $\bar{\nu}_{gs}$ decreases with increasing mass number of the target.

The average values of ν_{gs} , as well as the pre-saddle neutron multiplicity in the form of a range for the induced fission of the same target by different projectiles over the same projectile

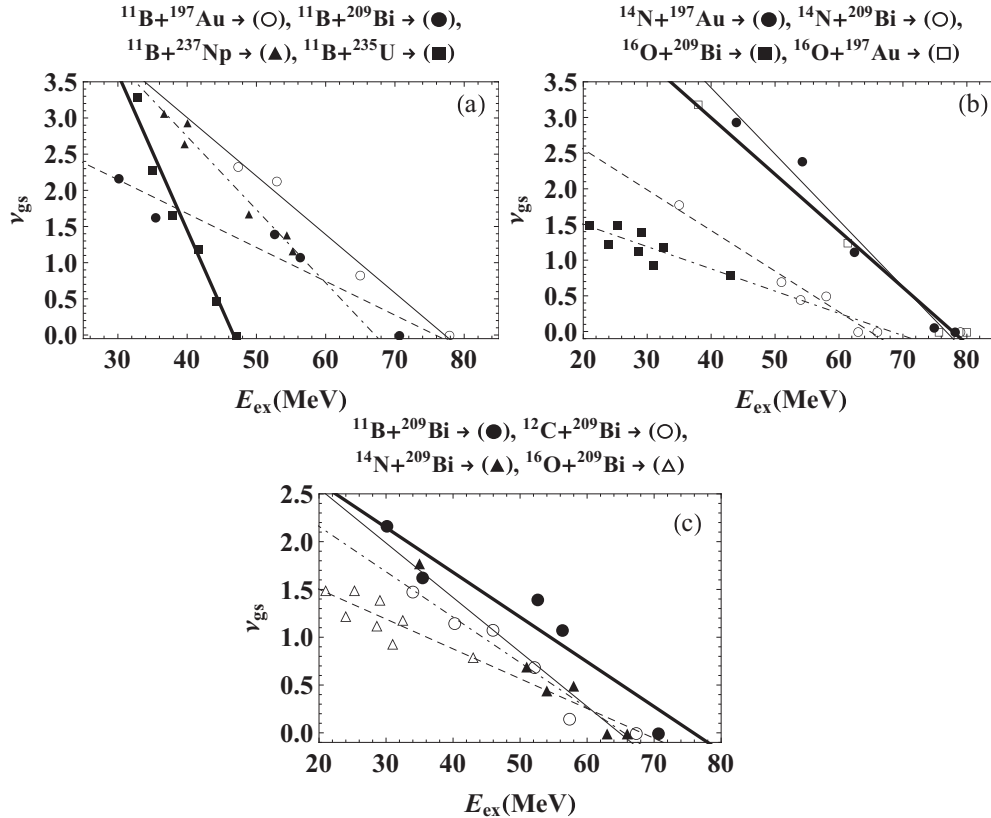


FIG. 3. Calculated pre-saddle neutron multiplicities. (a) For the $^{11}\text{B} + ^{197}\text{Au}$, ^{209}Bi , ^{235}U , ^{237}Np reaction systems. Thin solid, dashed, thick solid, and dash-dotted lines represent the general trends of the number of pre-saddle neutrons against the excitation energy of the compound nucleus, respectively. (b) For the ^{14}N , $^{16}\text{O} + ^{197}\text{Au}$ and ^{14}N , $^{16}\text{O} + ^{209}\text{Bi}$ reaction systems. Thin solid, thick solid, dashed, and dash-dotted lines represent the general trends of the number of pre-saddle neutrons against the excitation energy of the compound nucleus for these systems, respectively. (c) For the ^{11}B , ^{12}C , ^{14}N , $^{16}\text{O} + ^{209}\text{Bi}$ reaction systems. Thick solid, dash-dotted, thin solid, and dashed lines represent the general trends of the number of pre-saddle neutrons against the excitation energy of the compound nucleus for these systems, respectively.

TABLE II. Comparison between the calculated pre-saddle neutron multiplicity in the form of a range, as well as $\bar{\nu}_{gs}$ for fission reactions of the different targets induced by the same projectile.

Reaction systems	Projectile energy (units of $\frac{E_{c.m.}}{V_b}$)	ν_{gs}	$\bar{\nu}_{gs}$
$^{11}\text{B} + ^{197}\text{Au}$	1.4–1.9	3.1–1.4	2.0
$^{11}\text{B} + ^{209}\text{Bi}$	1.4–1.9	1.8–0.8	1.6
$^{12}\text{C} + ^{197}\text{Au}$	1.3–1.8	2.4–1.6	2.1
$^{12}\text{C} + ^{209}\text{Bi}$	1.3–1.8	1.5–0.4	1.0
$^{14}\text{N} + ^{197}\text{Au}$	1.2–1.7	3.0–0.5	1.9
$^{14}\text{N} + ^{209}\text{Bi}$	1.2–1.7	1.6–0.1	0.9
$^{16}\text{O} + ^{197}\text{Au}$	1.0–1.6	3.3–0.7	2.0
$^{16}\text{O} + ^{208}\text{Pb}$	1.0–1.6	1.9–0.1	1.5
$^{16}\text{O} + ^{209}\text{Bi}$	1.0–1.6	1.7–0.9	1.4

energy, are given in Table III. As can be seen in Table III, the quantity $\bar{\nu}_{gs}$ decreases with increasing mass number of projectile. All heavy-ion-induced reactions show that ν_{gs} falls quite rapidly with increasing mass asymmetry since it is partly due to a reduction of the dynamical fission time scale with the mass asymmetry.

We now attempt to estimate the pre-saddle neutron multiplicities in several fission reactions induced by light projectiles. We must pay attention to some important points that express the difference between fission induced by light projectiles and heavy ions. In fission induced by light projectiles, the energy in the center-of-mass framework $E_{c.m.}$ is roughly the same as that in the laboratory framework, and due to the low weight of the projectile, the rotational energy E_R can be neglected. Figure 4 shows calculated pre-saddle neutron multiplicities for the $\alpha + ^{182}\text{W}$ and $p + ^{185}\text{Re}$ reaction systems, which are leading to a similar ^{186}Os compound nucleus, as well as for the $p + ^{209}\text{Bi}$ and $\alpha + ^{206}\text{Pb}$ that formed the same ^{210}Po compound nucleus. For these systems, the experimental data of angular anisotropies are taken from the literature [49,50,59]. The values of $\langle I^2 \rangle$ for these systems are given by [49]

$$\langle I^2 \rangle = \frac{\sum(2I+1)T_I I(I+1)}{\sum(2I+1)T_I}, \quad (13)$$

TABLE III. Comparison between the calculated pre-saddle neutron multiplicity in the form of a range, as well as $\bar{\nu}_{gs}$ for fission reactions of the same target induced by different heavy ions.

Reaction systems	Projectile energy (units of $\frac{E_{c.m.}}{V_b}$)	ν_{gs}	$\bar{\nu}_{gs}$
$^{11}\text{B} + ^{209}\text{Bi}$	1.2–1.7	2.2–1.2	1.9
$^{12}\text{C} + ^{209}\text{Bi}$	1.2–1.7	1.8–0.8	1.2
$^{14}\text{N} + ^{209}\text{Bi}$	1.2–1.7	1.6–0.2	0.9
$^{16}\text{O} + ^{209}\text{Bi}$	1.2–1.7	1.4–0.6	0.8
$^{12}\text{C} + ^{197}\text{Au}$	1.2–1.6	2.8–1.8	2.4
$^{14}\text{N} + ^{197}\text{Au}$	1.2–1.6	3.0–1.0	2.3
$^{16}\text{O} + ^{197}\text{Au}$	1.2–1.6	2.5–0.7	2.0
$^{16}\text{O} + ^{208}\text{Pb}$	1.1–1.6	1.9–1.0	1.9
$^{19}\text{F} + ^{208}\text{Pb}$	1.1–1.6	1.4–0.4	1.4

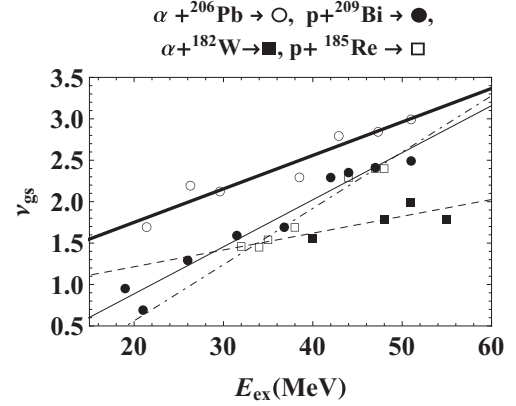


FIG. 4. The values of ν_{gs} for the $\alpha + ^{206}\text{Pb}$ and $p + ^{209}\text{Bi}$ reaction systems, which are leading to the same ^{210}Po compound nucleus, as well as for the $\alpha + ^{182}\text{W}$, and $p + ^{185}\text{Re}$ reaction systems that formed the same ^{186}Os compound nucleus. Thick solid, thin solid, dashed, and dash-dotted lines represent the general trends of the pre-saddle neutrons against the excitation energy of the compound nucleus for these systems, respectively.

where T_I are the entrance channel transmission coefficients and satisfy $T_I = 1$ for $I \leq I_{max}$ and $T_I = 0$ for $I > I_{max}$. If the maximum angular momentum is determined by the relation $\langle I^2 \rangle = 1/2I_{max}^2$, the following relations give the values of the mean square angular momentum of the compound nucleus for the fission of pre-actinide nuclei induced by proton and α particles, respectively:

$$\langle I^2 \rangle = 2.08E_p(\text{MeV}) - 15, \quad (14)$$

$$\langle I^2 \rangle = 10.2E_\alpha(\text{MeV}) - 199. \quad (15)$$

In heavy-ion-induced fission at low bombarding energies, several neutrons are evaporated prior to reaching the saddle point, and at the highest bombarding energy, essentially all the neutrons are evaporated by the fission fragments; i.e., the fission process is rapid compared to the time scale for neutron evaporation. However, the number of pre-saddle neutrons ν_{gs} increases with increasing excitation energy of the compound nucleus in fission induced by light projectiles. This behavior is mainly because in the fission induced by light projectiles, the fission barrier height is higher than the neutron binding energy and B_f is approximately independent of the excitation energy of the compound nucleus. Therefore the fission probability $P_f = \frac{\Gamma_f}{\Gamma_{tot}}$ is negligible at low energies. When $E_{ex} < B_f$, it is impossible for the compound nucleus to undergo fission, but there is sufficient excitation energy to emit several neutrons. It is clear that fission becomes significant if $E_{ex} > B_f$.

IV. SUMMARY AND CONCLUSIONS

We have presented the calculated pre-saddle neutron multiplicities for several heavy-ion-induced fission reactions, as well as for several fission reactions induced by light projectiles. The calculation using the experimental data of fission-fragment angular anisotropies as well as the prediction of the SSPSM is a novel method, which has been carried out in this work for the first time. We have also considered

the behavior of pre-saddle neutron multiplicities in fission reactions induced by heavy ions and light projectiles. In heavy-ion-induced fission, the number of pre-saddle neutrons decreases with increasing excitation energy of the compound nucleus. However, in fission induced by light particles, the number of pre-saddle neutrons increases with increasing excitation energy of the compound nucleus. The fission barrier height in heavy-ion fission reactions depends on the excitation energy of the compound nucleus. On the other hand, the fission barrier height [and thus ground-to-saddle transition time, $\tau_{gs} \propto \ln(10B_f/T)$] decreases with increasing excitation energy of the compound nucleus. As a result, in heavy-ion-induced fission the number of pre-saddle neutrons decreases with increasing excitation energy of the compound nucleus. Our results also show that the emission rate of neutrons is approximately constant in the transition from the ground state to the saddle point and then from the saddle to the scission points. On the contrary, in fission induced by light projectiles, the fission barrier height is greater than the neutron binding energy, and the fission barrier is approximately independent of the excitation energy. Hence the compound nucleus does not

undergo fission unless the excitation energy of the compound nucleus exceeds the fission barrier. As a result, in fission induced by light projectiles, the number of pre-saddle neutrons exhibits an increasing function against the excitation energy of the compound nucleus, as shown by our calculations. The number of pre-saddle neutrons for reactions leading to the same compound nucleus at any given excitation energy appears to be nearly equal since the number of pre-saddle neutrons depends only on the mass of the compound nucleus and it is independent of the entrance mass asymmetry parameter. This behavior of the number of the pre-saddle neutrons as a function of the projectile mass and/or of the target mass may also be related to the size of compound nucleus. We observe that the average number of pre-saddle neutrons decreases with an increasing mass number of projectiles in fission reactions of the same target induced by different projectiles. A similar behavior in the multiplicities of pre-saddle neutrons is also observed in fission reactions of different targets induced by the same projectile. In the end, our results may provide useful information on the ground-state-to-saddle and saddle-to-scission transition times.

-
- [1] A. Gavron, J. R. Beene, B. Cheynis, R. L. Ferguson, F. E. Obenshain, F. Plasil, G. R. Young, G. A. Pettit, M. Jääskeläinen, D. G. Sarantites, and C. F. Maguire, *Phys. Rev. Lett.* **47**, 1255 (1981).
- [2] E. Holub, D. Hilscher, G. Ingold, U. Jahnke, H. Orf, and H. Rossner, *Phys. Rev. C* **28**, 252 (1983).
- [3] W. P. Zank, D. Hilscher, G. Ingold, U. Jahnke, M. Lehmann, and H. Rossner, *Phys. Rev. C* **33**, 519 (1986).
- [4] D. J. Hinde, R. J. Charity, G. S. Foote, J. R. Leigh, J. O. Newton, S. Ogaza, and A. Chatterjee, *Phys. Rev. Lett.* **52**, 986 (1984).
- [5] A. Gavron, A. Gayer, J. Boissevain, H. C. Britt, T. C. Awes, J. R. Beene, B. Cheynis, D. Drain, R. L. Ferguson, F. E. Obenshain, F. Plasil, G. R. Young, G. A. Pettitt, and C. Butler, *Phys. Rev. C* **35**, 579 (1987).
- [6] D. J. Hilscher, H. Rossner, B. Cramer, B. Gebauer, U. Jahnke, M. Lehmann, E. Schwinn, M. Wilpert, Th. Wilpert, H. Froeben, E. Mordhorst, and W. Scobel, *Phys. Rev. Lett.* **62**, 1099 (1989).
- [7] D. J. Hinde, D. Hilscher, H. Rossner, B. Gebauer, M. Lehmann, and M. Wilpert, *Phys. Rev. C* **45**, 1229 (1992).
- [8] H. Rossner, D. J. Hinde, J. R. Leigh, J. P. Lestone, J. O. Newton, J. X. Wei, and S. Elfström, *Phys. Rev. C* **45**, 719 (1992).
- [9] A. Saxena, A. Chatterjee, R. K. Choudhury, S. S. Kapoor, and D. M. Nadkarni, *Phys. Rev. C* **49**, 932 (1994).
- [10] E. Duek, N. N. Ajitanand, John M. Alexander, D. Logan, M. Kildir, L. Kowalski, Louis C. Vaz, D. Guerreau, M. S. Zisman, Morton Kaplan, and D. J. Moses, *Z. Phys. A* **317**, 83 (1984).
- [11] J. O. Newton, *Sov. J. Part. Nucl.* **21**, 349 (1990); *Pramana J. Phys.* **39**, 175 (1989).
- [12] S. S. Kapoor, in International Nuclear Data Committee, Report INDC(NDS)-220, 1989, p. 221 (unpublished).
- [13] J. O. Newton, D. J. Hinde, R. J. Charity, J. R. Leigh, J. J. M. Bokhorst, A. Chatterjee, G. S. Foote, and S. Ogaza, *Nucl. Phys. A* **483**, 126 (1988).
- [14] M. Streckler, R. Wien, P. Plischke, and W. Scobel, *Phys. Rev. C* **41**, 2172 (1990).
- [15] D. J. Hinde, H. Ogata, M. Tanaka, T. Shimoda, N. Takahashi, A. Shinohara, S. Wakamatsu, K. Katori, and H. Okamura, *Phys. Rev. C* **39**, 2268 (1989).
- [16] E. Cheifetz, Z. Fraenkel, J. Galin, M. Lefort, J. Peter, and X. Tarrago, *Phys. Rev. C* **2**, 256 (1970).
- [17] A. Gavron, A. Gayer, J. Boissevain, H. C. Britt, J. R. Nix, A. J. Sierk, P. Grange, S. Hassani, H. A. Weidenmuller, J. R. Beene, F. Plasil, G. R. Young, G. A. Pettitt, and C. Butler, *Phys. Lett. B* **176**, 312 (1986).
- [18] D. Hilscher and H. Rossner, *Ann. Phys. (Paris, Fr.)* **17**, 471 (1992).
- [19] N. Bohr and J. A. Wheeler, *Phys. Rev.* **56**, 426 (1939).
- [20] M. Thoennessen and G. F. Bertsch, *Phys. Rev. Lett.* **71**, 4303 (1993).
- [21] P. Fröbrich and H. Rossner, *Z. Phys. A* **349**, 99 (1994).
- [22] P. Fröbrich, I. I. Gontchar, and N. D. Mavlitov, *Nucl. Phys. A* **556**, 281 (1993).
- [23] P. Fröbrich and I. I. Gontchar, *Nucl. Phys. A* **563**, 326 (1993).
- [24] P. N. Nadtochy, G. D. Adeev, and A. V. Karpov, *Phys. Rev. C* **65**, 064615 (2002).
- [25] P. N. Nadtochy, E. G. Ryabov, A. E. Gegechkori, Yu. A. Anischenko, and G. D. Adeev, *Phys. Rev. C* **85**, 064619 (2012).
- [26] R. Rafiei, R. G. Thomas, D. J. Hinde, M. Dasgupta, C. R. Morton, L. R. Gasques, M. L. Brown, and M. D. Rodriguez, *Phys. Rev. C* **77**, 024606 (2008).
- [27] B. P. Ajith Kumar, K. M. Varier, R. G. Thomas, K. Mahata, B. V. John, A. Saxena, H. G. Rajprakash, and S. Kailas, *Phys. Rev. C* **72**, 067601 (2005).
- [28] R. Tripathi, K. Sudarshan, A. Goswami, P. K. Pujari, B. S. Tomar, and S. B. Manohar, *Phys. Rev. C* **69**, 024613 (2004).
- [29] S. Soheyl, *Phys. Rev. C* **84**, 044609 (2011).
- [30] R. Tripathi, K. Sudarshan, S. Sodaye, S. K. Sharma, and A. V. R. Reddy, *Phys. Rev. C* **75**, 024609 (2007).
- [31] E. Prasad *et al.*, *Phys. Rev. C* **81**, 054608 (2010).

- [32] S. Appannababu, S. Mukherjee, N. L. Singh, P. K. Rath, G. K. Kumar, R. G. Thomas, S. Santra, B. K. Nayak, A. Saxena, R. K. Choudhary, K. S. Golda, A. Jhingan, R. Kumar, P. Sugathan, and H. Singh, *Phys. Rev. C* **80**, 024603 (2009).
- [33] B. P. Ajitkumar, K. M. Varier, B. V. John, A. Saxena, B. K. Nayak, D. C. Biswas, R. G. Thomas, and S. Kailas, *Phys. Rev. C* **77**, 021601(R) (2008).
- [34] G. N. Knyazheva *et al.*, *Phys. Rev. C* **75**, 064602 (2007).
- [35] R. Tripathi, K. Sudarshan, S. Sodaye, A. V. R. Reddy, K. Mahata, and A. Goswami, *Phys. Rev. C* **71**, 044616 (2005).
- [36] R. Vandenbosch and J. R. Huizenga, *Nuclear Fission* (Academic, New York, 1973).
- [37] M. B. Tsang, D. Arduoin, C. K. Gelbke, W. G. Lynch, Z. R. Xu, B. B. Back, R. Betts, S. Saini, P. A. Baisden, and M. A. McMahan, *Phys. Rev. C* **28**, 747 (1983).
- [38] A. J. Sierk, *Phys. Rev. C* **33**, 2039 (1986).
- [39] J. Fernandez-Niello, C. H. Dasso, and S. Landowne, *Comput. Phys. Commun.* **54**, 409 (1989).
- [40] T. D. Thomas, *Phys. Rev.* **116**, 703 (1959).
- [41] C. Y. Wong, *Phys. Rev. Lett.* **31**, 766 (1973).
- [42] T. Udagawa, B. T. Kim, and T. Tamura, *Phys. Rev. C* **32**, 124 (1985).
- [43] H. Esbensen, *Nucl. Phys. A* **352**, 147 (1981).
- [44] R. Vandenbosch, *Annu. Rev. Nucl. Part. Sci.* **42**, 447 (1992).
- [45] S. Soheyli and M. K. Khalili, *Phys. Rev. C* **85**, 034610 (2012).
- [46] V. E. Viola, J. T. D. Thomas, and G. T. Seaborg, *Phys. Rev.* **129**, 2710 (1963).
- [47] E. Vulgaris, L. Grodzins, S. G. Steadman, and R. Ledoux, *Phys. Rev. C* **33**, 2017 (1986).
- [48] B. R. Behera, S. Kailas, K. Mahata, A. Chatterjee, P. Basu, S. Roy, M. Satpathy, and S. K. Datta, *Nucl. Phys. A* **734**, 249 (2004).
- [49] A. V. Ignatyuk, M. G. Itkis, I. A. Kamenev, S. I. Mulgin, V. N. Okolovich, and G. N. Smirenkin, *Sov. J. Nucl. Phys.* **40**, 400 (1984).
- [50] S. D. Beizin, M. G. Itkis, I. A. Kamenev, S. I. Milgin, V. N. Okolovich, and G. N. Smirenkin, *Sov. J. Nucl. Phys.* **43**, 883 (1986).
- [51] D. J. Hinde, *Nucl. Phys. A* **553**, 255c (1993).
- [52] C. J. Bishop, I. Halpern, R. W. Shaw, Jr., and R. Vandenbosch, *Nucl. Phys. A* **198**, 161 (1972).
- [53] S. Hassani and P. Grange, *Phys. Lett. B* **137**, 281 (1984).
- [54] Z. Liu, H. Zhang, J. Xu, Y. Qiao, X. Qian, and C. Lin, *Phys. Rev. C* **54**, 761 (1996).
- [55] R. Vandenbosch, J. D. Bierman, J. P. Lestone, J. F. Liang, D. J. Prindle, A. A. Sonzogni, S. Kailas, D. M. Nadkarni, and S. S. Kapoor, *Phys. Rev. C* **54**, R977 (1996).
- [56] S. Kailas, D. M. Nadkarni, A. Chatterjee, A. Saxena, S. S. Kapoor, R. Vandenbosch, J. P. Lestone, J. F. Liang, D. J. Prindle, A. A. Sonzogni, and J. D. Bierman, *Phys. Rev. C* **59**, 2580 (1999).
- [57] B. B. Back, R. R. Betts, J. E. Gindler, B. D. Wilkins, S. Saini, M. B. Tsang, C. K. Gelbke, W. G. Lynch, M. A. McMahan, and P. A. Baisden, *Phys. Rev. C* **32**, 195 (1985).
- [58] B. R. Behera, M. Satpathy, S. Jena, S. Kailas, R. G. Thomas, K. Mahata, A. Chatterjee, S. Roy, P. Basu, M. K. Sharan, and S. K. Datta, *Phys. Rev. C* **69**, 064603 (2004).
- [59] A. V. Ignatyuk, M. G. Itkis, I. A. Kamenev, S. I. Mulgin, V. N. Okolovich, Yu. B. Ostapenko, and G. N. Smirenkin, *Sov. J. Nucl. Phys.* **40**, 892 (1984).